IRANIAN JOURNAL OF PHYSICS RESEARCH

Iranian Journal of Physics Research, Vol. 14, No. 3, 2014

Influence of shielding gas composition on weld profile in pulsed Nd:YAG laser welding of low carbon steel

M Jokar[1], F MalekGhaini[1], M J Torkamany[1,2] and M Sheikhi[1]

1. Department of Materials Engineering, Tarbiat Modares University, Tehran, Iran
2. Iranian National Center for Laser Science and Technology, Tehran, Iran
E-mail: fmalek@modares.ac.ir

(Received 12 May 2013 , in final from 31 October. 2013)

Abstract

Weld area and weld depth/width ratio can be considered to be of the most important geometrical factors in pulsed laser welding. The effects of carbon dioxide and oxygen additions to the argon shielding gas on the weld properties in pulsed laser welding of low carbon steel is investigated. Presence of carbon dioxide and oxygen up to 10 and 15 percent respectively decreases the weld geometrical factors. But, at higher levels of additions, the weld geometrical factors will increase. It is observed that the plasma plume temperature decreases from 6000K to 5500K with the addition of 15% carbon dioxide but increases to 7700K with 25% carbon dioxide addition. Increase in laser absorption coefficient, laser energy absorption, formation of oxide layer on the work-piece surface, exothermic reactions and their competitive effects can be considered as the competing phenomena involved in such a behavior in the weld profile.

Keywords: weld area, weld depth/width ratio, laser welding, shielding gas, weld profile, plasma plume

1. Introduction

In laser welding, shielding gas which is fed into the weld area by a coaxial or a side nozzle has the duty of protecting the laser optics from the weld spatter, protecting the weld pool against the atmosphere, and improving the coupling of laser-material [1, 2]. It is well known that a portion of the laser energy is expended in ionizing the shielding gas and the metal vapors coming from the base material. Thus, the plasma contains both ionized and excited atoms of substrate and shielding gas [3, 4]. Properties of plasma plume depend on the type of shielding gas, base metal, and energy density [5]. Plasma generated in laser welding is often assumed to be optically thin (electron density between 1014 and 1018 cm^{-3}) and in local thermodynamic equilibrium (LTE) [6]. Plasma is said to be in LTE when particles have Maxwellian energy distribution, and collisional de-excitations dominate the radioactive de-excitations [6]. According to the theory of atomic emission spectroscopy, the plasma temperature is generally estimated by the relative emission intensities of spectral lines. The use of emission spectroscopy in order to study the characteristics of plasma plume formed during laser welding and investigation of effects of shielding gas parameter on plasma properties have been the subject of the study by Sabaghzadeh *et al*. [7] who investigated pulsed Nd:YAG laser welding of a low carbon steel sheet metal and found that the plasma temperature decreased by increasing the gas flow rate. Jandaghi and co-worker [8-10] calculated the vaporization rates and Weld metal composition change during pulsed Nd:YAG laser welding using laser-induced plasma spectroscopy. Dadras *et al*. [11] investigated pulsed Nd:YAG laser welding of a copper-nickel alloy sheet metal and found that plasma temperature is increased by enhancing metal absorptivity when O_2 is used as the shielding gas. The effects of different volume ratios of He and Ar in shielding gas during Nd:YAG and CO_2 laser welding were studied by Hosseini Motlagh *et al*. [12] who solved the Saha equations for two-component mixtures. Although the effect of the shielding gas composition has been the subject of several studies on CO_2 laser welding, it seems that there are many unclear points in pulsed Nd:YAG laser welding yet. Abbott *et al*. [13] studied the effects of helium, argon and carbon dioxide shielding gases on the shape of the plasma plume of a CO_2 laser. Chung and co-worker [14] found that when carbon dioxide is used as shielding gas in CO_2 laser welding of iron, because of the lower dissociation ionization

Table 1. The chemical composition of the steel plate.

C (wt.)	Si (wt.%)	Mn (wt.%)	P (wt.%)	S (wt.%)
0.04	0.004	0.22	0.006	0.006

potential of carbon dioxide, the upper plasma was mainly constituted of carbon monoxide ions and less iron ions. Reisgen *et al*. [15] have investigated the effect of shielding gas on the shape and formability of carbon steel sheet metal welds made with CO_2 laser, and showed that a mixture of 50% argon +50% nitrogen gives the optimum result considering production cost, formability, and penetration depth. It is generally known that, during laser welding of metals or steel alloys, the protective/shielding gas is normally applied to decrease the oxygen content within the working area. While, interaction time of the melt material in pulsed Nd:YAG laser welding is shorter than other conventional welding process [16]. So, it is expected that the negative effects of the reactive gases on weld metal properties would be limited. However, systematic reports on the effects of shielding gas composition in pulsed Nd:YAG laser welding of steel alloys are very limited [17]. The question is that regarding the formation of surface oxide layers in the presence of reactive gases (like O_2 and CO_2) that improves laser absorption and exothermic reaction of these gases with iron [13, 14], can we add some controlled percentage of reactive gases to the shielding gas?. The prime objective of this research is to improve the understanding of laser–material interaction using additions of CO_2 and O_2 to argon gas, in the scope of a low power pulsed Nd:YAG laser as applied to welding thin automotive low carbon steel. Weld area and weld depth/width ratio can be considered to be of the most important geometrical factors in fusion welding specially in pulsed laser welding. It is hoped that this endeavor will help to further exploit the potential of this modern welding process in the ever increasing applications.

2. Method

Low carbon steel plate (Grade ST 14) with a thickness of 2 mm was used as a substrate for the experiments.Chemical composition of the base metal is given in table 1. Prior to welding, surface of the plate was ground using a 180-grit abrasive paper and then cleaned by acetone. A pulsed Nd:YAG laser (IQL-10 model) with a maximum average power of 400 Watt was used to make bead on plate welds.

A set of Rotameter flow meters was used to measure the shielding gas flow rate. The coaxial shielding gas nozzle with a 5 mm diameter was positioned at 2 mm distance from the work-piece surface. CO_2 and O_2 gases were added to argon gas according to table 2.

In order to avoid inadvertent welding condition (such as too much spatter or porosity), an initial series of experiments were performed and the following parameters were found to give reasonably sound welds and shapes making it possible to focus on the effect of shielding gas composition on weld profile. The parameters were: pulse energy at 11 J, pulse duration at 7 ms, pulse frequency 20 s^{-1}, travel speed 4 mm/s, and shielding gas flow rate 60 lit/min. To study the weld dimensions and microstructure, the weld beads were cut, polished, and etched with 2% nital solution. Emission spectroscopy method was used to determine the plasma temperature. Emission spectra from the laser induced plasma were measured with an EPP2000-UV model StellarNet Inc. spectrometer constructed from 1200 gmm^{-1} holographic-plane grating, a 2_1024 element CCD detector, and a 10 mm slit, which led to the instrument having 0.4 nm resolution in the 200–600 nm wavelength interval. The emitted light of the plasma plume was entered into the spectrometer by a thermally resistant optical fiber.

Table 2. Chemical composition of shielding gas.

Weld sample codes	Additive gas to argon	Volume percent of additive (sample 1 to 6)
A_1 to A_6	CO_2	0, 5, 10, 15, 20, 25
B_1 to B_6	O_2	0, 6, 8, 10, 12, 14

3. Results

Figure 1 shows typical weld profiles obtained through addition of CO_2 to argon.

The results of weld profile measurements as a function of shielding gas composition are illustrated for weld area and weld depth/width ratio in figures 2 and 3, respectively.

It can be seen that in the presence of CO_2 gas up to 15% and O_2 up to 10% in argon, the melt area and depth/width ratio of the welds are decreased. However, at higher levels of either CO_2 or O_2, both the melt area and the depth/width ratio of the welds are increased. Emission spectra were measured to determine the plasma temperature. The temperature of the plasma plume formed above the melt pools during laser welding can be measured by investigating the relative intensities of the spectral lines [18]. The governing equation is:

$$\ln\left(\lambda I / A g_u\right) = c - (E_u / kT) \quad , \tag{1}$$

where I, λ, A, g_u, E_u, k and T are the relative intensity, wavelength, the transition probability, the statistical weight of the upper level, the energy of the upper level, Boltzmann's constant and temperature, respectively.

In order to increase the accuracy of plasma temperature measurement, different spectrum lines of the main part of plasma can be selected. The form of equation (1) is $y = mx + c$, so a graph of $\ln\left(\lambda I / A g_u\right)$ against E_u will be a straight line, with the slope of $(m = -1/kT)$, or:

$$T = -1/km \quad . \tag{2}$$

Figure 4 shows the typical spectrum lines of the plasma.

The selected FeI lines and their quantum mechanical features are listed in table 3. Figure 5 shows the calculated plasma electron temperature for A_1 (100%Ar), A_4 (15% CO_2+ 85%Ar), and A_6 (25% CO_2+ 75%Ar) samples together with the corresponding weld profile

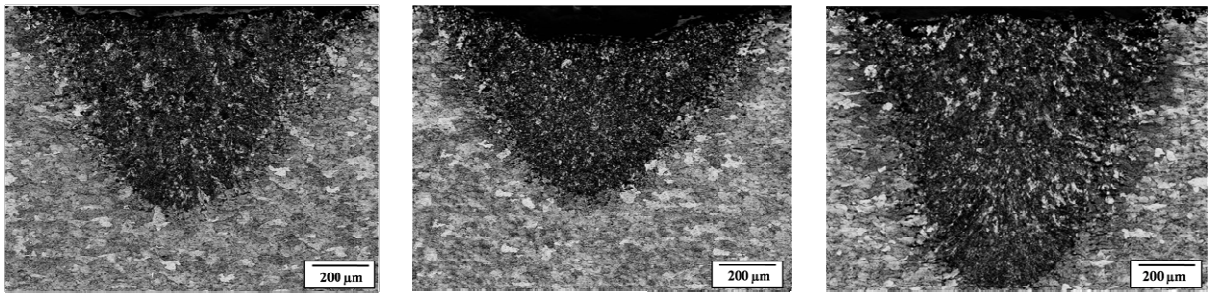

a b c

Figure 1.Welds produced with different mixtures of argon and carbon dioxide: (a) A_1 (100% Ar), (b) A_4 (85% Ar + 15% CO_2), (c) A_6(75% Ar + 25% CO_2).

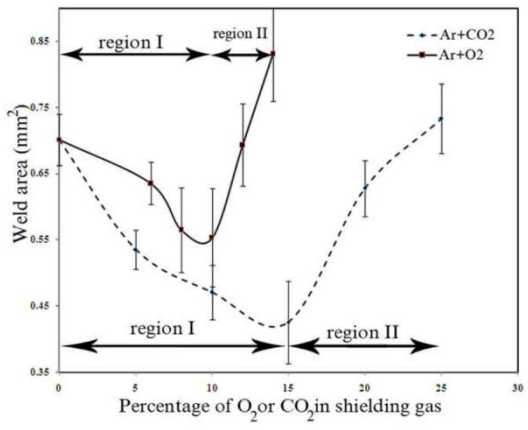

Figure 2. Weld area versus CO_2 or O_2 concentration in shielding gas.

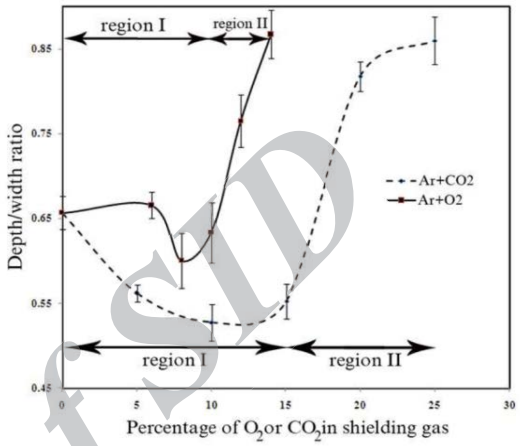

Figure 3. Weld depth/width ratio versus CO_2 or O_2 concentration in shielding gas.

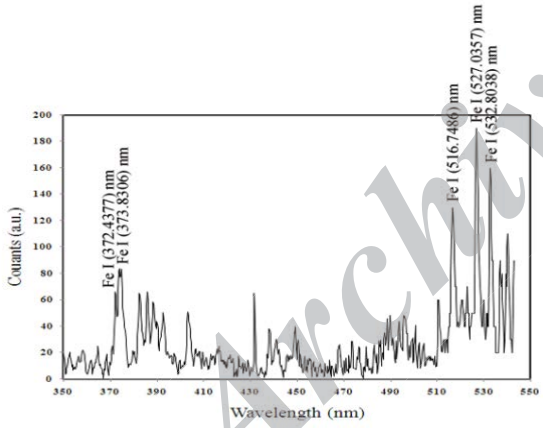

Figure 4. Typical spectrum lines of the plasma.

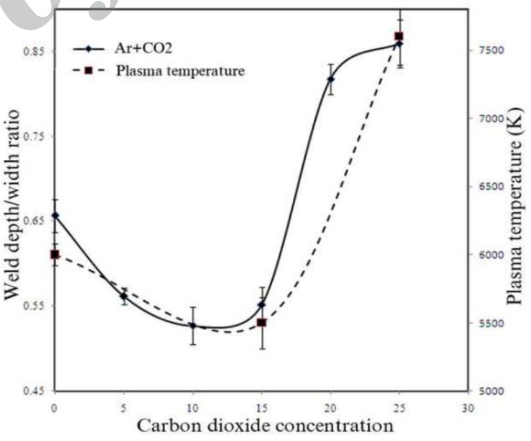

Figure 5. Effect of carbon dioxide concentration in argon shielding gas on the calculated plasma temperature and weld profile.

Table 3. Selected emission lines of Fe I for calculation of the electron temperature [19].

λ (nm)	E_u (cm^{-1})	g_u	A (10^8 s^{-1})
372.4377	45226.76	7	1.3×10^{-1}
373.8306	53093.521	13	3.8×10^{-1}
516.7487	31322.611	7	2×10^{-2}
527.0357	31937.316	3	2.5×10^{-2}
532.8038	26140.177	7	1.15×10^{-2}

parameters. Figure 5 shows that the calculated plasma temperature can be correlated with depth/width ratio of the welds.

4. Discussion

The results clearly indicate that in pulsed Nd:YAG laser welding of low carbon steel, addition of CO_2 or O_2 to Argon shielding gas can affect the weld pool dimensions significantly. However, Figures 2 and 3 show that the effect is complex as the trend in weld profile changes direction with increased addition of CO_2 or O_2. The shielding gas composition can affect the weld pool shape through three major processes: inverse Bremsstrahlung

Table 4. Characteristic properties of shielding gas elements and base material (NIST,www.nist.gov/)

material	ionization potential (eV)	dissociation energy (eV)	atomic weight (g/mol)
Ar	15.75	-	39.95
CO_2	13.77	5.5	44
O_2	12.07	6.66	32
Fe	7.90	-	55.85

effect (IB), Marangoni convection in the melted metal, and laser absorption by surface. The final weld profile can be regarded as coupling or competition of the above mentioned processes. Generally, in laser welding processes, a portion of the laser energy is absorbed by the plasma through the IB heating i.e. absorption of photons energy by charged particles through collisions [20]. During Nd:YAG laser welding although this phenomenon is less important because of lower laser wavelength, it will affect the characteristics of the heat pumped into the weld pool, and indeed can change the profile and properties of the weld produced [16]. The IB absorption coefficient is expressed as follows [21]:

$$\alpha_w = \frac{z^2 n_e n_i e^6 \ln A}{3\varpi^2 c \varepsilon_0^3 (2\pi m_e k T_e)^{3/2} \sqrt{1-\left(\omega_p/\omega\right)^2}} \quad , \qquad (3)$$

where n_e and n_i are respectively the electron and ion number density (m^{-3}), z is the charge number, e is the electronic charge (C), c is the light velocity ($m.s^{-1}$), ε_0 is the dielectric constant ($F.m^{-1}$), m_e is the mass of the electron (kg), k denotes the Boltzmann constant ($J.K^{-1}$), T_e is the plasma temperature (K), ω is the angular frequency of the incident wave (s^{-1}), ω_p is the angular frequency of plasma oscillation (s^{-1}), and ln A is the Coulomb logarithm. Ion density of plasma in the LTE condition can be described by Saha's equation [3]:

$$\frac{n_e n_i}{n_o} = \frac{g_i g_e (2\pi k m_e T_e)^{3/2}}{g_o h^3} \exp\left[\frac{-E_i}{kT_e}\right] , \qquad (4)$$

where n_e, n_i and n_o are the densities of electrons, ions and neutral atoms, respectively. g_e, g_i and g_o represent the degeneracy factors of electrons, ions and neutral atoms respectively, h Plank's constant (J.s) and E_i is the ionization potential for the neutral atoms (J). Table 4 shows ionization potential, dissociation energy and atomic weight of shielding gas components and the base material used in this survey. When carbon dioxide and oxygen are added to the shielding gas, the amount of total ionization potential (E_i) in equation (4) decreases as a result of lower dissociation and ionization energies of CO_2 and O_2 molecules in comparison with ionization energy of argon (as seen in table 4).

Therefore electron and ions densities (n_e and n_i) of the plasma plume would increase by adding the above mentioned reactive gases to the argon shielding gas. Thus, increasing the electron density can increase the IB absorption as presented in equation (3). In a theoretical model developed by Glowacki [6] the density of singly ionized atoms and IB coefficient as a function of temperature for argon+nitrogen compositions in CO_2 laser welding were calculated showing that by adding nitrogen, ions density and IB absorption would increase, due to lower dissociation and ionization energy of nitrogen with respect to the ionization energy of argon. Increasing the plasma plume absorption coefficient through IB effect will result in decreasing the energy received by the work-piece surface. So, by adding fractional amount of reactive gases to the argon shielding gas, a decrease in the irradiated energy is expected to occur and that in turn can result in a decrease in the heat input to the work-piece. Finally, it is inferred that by adding low amounts of reactive additive to the shielding gas the plasma plume temperature decreases, IB absorption coefficient and refractive index of the plasma increase. All of these phenomena have lowered the laser beam energy transmitted through the plume and can result in decreasing the area and depth/width ratio of the melt pool at lower amounts of CO_2 and O_2. Adsorption of oxygen ions in the weld pool during the welding process can occur because of generation of O^+ and O_2^+ ions from dissociation and ionization reaction of CO_2 and O_2 molecules in the plasma plume. While the reactions occurring during laser welding are not in the equilibrium condition, the assumptions based on equilibrium condition can be used for the prediction of reaction directions. Adsorption of oxygen in the weld pool during the welding process can be expressed as follows [22]:

(i) for monatomic oxygen ions (O^+):

$$O^+ + e^- = O(g) \quad , \qquad (5)$$

$$O(g) = O(\text{in melt pool}) \qquad (6)$$

$$\Delta G_{\text{solution } O(g)} < \Delta G^0_{\text{solution } O(g)} - RT \ln(P_{O(g)}) \qquad (7)$$

(ii) for diatomic oxygen ion (O_2^+):

$$O_2^+ + e^- = O_2(g) \quad , \qquad (8)$$

$$O_2(g) = 2O \ (\text{in melt pool}) \qquad (9)$$

$$\Delta G_{\text{solution } O_2(g)} < \Delta G^0_{\text{solution } O_2(g)} - RT \ln(P_{O_2(g)}) \qquad (10)$$

where ΔG is the Gibbs free energy, ΔG^0 is the standard Gibbs free energy, R is the universal gas constant, T is the temperature and $P_O(g)$ and $P_{O2}(g)$ are the partial pressure of monatomic and diatomic oxygen gas, respectively. For the progress of each reaction, the Gibbs free energy must be lower than zero.

Therefore, in equations (7) and (10), partial pressure of monatomic and diatomic oxygen gas in plasma plume must be higher than $\left(e^{\frac{\Delta G^0_{\text{solution } O(g)}}{RT}}\right)$ and $\left(e^{\frac{\Delta G^0_{\text{solution } O_2(g)}}{RT}}\right)$, respectively.

Figure 6. Surface appearance of *A* series: (a) A_1 (100% Ar), (b) A_4 (85% Ar + 15% CO_2), (c) A_6 (75% Ar +25% CO_2).

Since the oxygen content in "region II" of Figure 2 is higher, the possibility of dissolution of oxygen in this region increases and accordingly more oxide can be formed on the weld pool surface. Surface appearances of the A series of experiments are shown in figure 6.

When concentration of CO_2 in shielding gas is lower than 15% the weld surface is relatively clean, as can be seen in figure 6(a) and (b). However, when the CO_2 percentage in the shielding gas increases to 25%, a continuous oxide layer covers the weld surface as shown in figure 6(c). Similar results were obtained when O_2 was added to the argon as shielding gas. Surface absorptivity is highly dependent on a variety of parameters like surface temperature and surface conditions [23]. As mentioned above, increase in the presence of iron oxide on the melt surface can result in an increase in the absorption of the laser energy. Therefore heat input to weld pool would increase. On the other hand, the energy released from oxidation reaction may contribute to increasing the effective heat input to the melt pool. Consequently in "region II" creation of surface oxide layer will compensate for the effect of plasma absorption coefficient (IB) and results in increasing the melt pool dimensions.

Marangoni convection is another process that can affect the shape of the melt pool [24]. Generally the surface tension of many materials decreases by increasing the temperature. In other words, surface tension of the cooler parts is higher. Hence, the liquid metal flows from warmer liquid parts in the center to the cooler zones at the edge of the weld pool [25]. If a relatively small amount of surface active elements such as oxygen is present, variation of the surface tension with temperature will alter from negative to positive. In this situation, the cooler liquid metal at the edges of the melt pool is pulled by the warmer parts of liquids in center and the weld pool tends to become narrow and deep [26, 27]. Therefore in "region II" of figure 3 the presence of oxygen on top of the weld pool surface can change the direction of the Marangoni convection and result in increasing the depth/width ratio of the melt pool. Lu and co-worker [25-27] investigated the effects of O_2 and CO_2 additions to shielding gas on the weld shape of SUS304 stainless steel in gas tungsten arc welding (GTAW) and showed that when the oxidizing content in shielding gas is higher than a critical value, weld depth/width ratio would increase. It is interesting to note that figures 2 and 3 show that the effects of CO_2 in argon shielding gas on the weld profile do follow a trend similar to that of O_2 but at a higher volume percentage. Kuwana and Sato [28] studied the effects of Ar–O_2, Ar–CO_2 and Ar–O_2–CO_2 shielding gases on the oxygen absorption of pure iron in gas metal arc welding (GMAW). They showed that the weld metal oxygen absorption content under Ar–O_2 is higher than that under Ar–CO_2 shielding gas, due to lower oxidation ability of CO_2 with respect to O_2. The comparative additional gas in the mixtures for the minimum weld metal area to occur can be deduced from figure 2 which is about 15% for CO_2 and 10% for O_2, i.e. 3 to 2. This ratio is also that of oxygen atoms in O_2 to that in CO_2 molecules. The above observation supports the proposition that at least in terms of the weld profile, it is oxygen which plays the primary role in the interaction of the plasma and the molten metal for the mixtures of argon and either CO_2 or O_2 as shielding gas in Nd:YAG pulsed laser welding of thin carbon steel plates.

5. Conclusions

The weld profile in pulsed Nd: YAG laser welding of carbon steel plate is affected by shielding gas composition. Adding small percentages of CO_2 and O_2 reactive gases to the argon shielding gas decreases the weld area and depth/width ratio in the weld profile. However, higher percentages of CO_2 and O_2 will increase the melt pool dimensions and the upper keyhole plasma temperature. Maximum amounts of the weld area and depth/width ratio are obtained at 25% CO_2 and 14% O_2. In terms of the weld profile, it seems that oxygen plays the major role in the interaction of the laser induced plasma and the molten metal in cases that a mixtures of argon and either CO_2 or O_2 are used as shielding gas.

Acknowledgements

The authors would like to thank Mr A Chehreghani and M J Hamedi, for their technical assistance.

References

1. A Ancona, T Sibillano, L Tricarico, R Spina, P M Lugara, G Basile, and S Schiavone, *Journal of Materials Processing Technology* **164–165** (2005) 971.
2. R Li, Z Li, Y Zhu, and L Rong, *Materials Science and Engineering* A **528** (2011) 1138.
3. Y Zhang, L Li, and G Zhang, *Journal of Physics* D: *Applied Physics* **38** (2005) 703.

4. H Wang, Y Shi, S Gong, and A Duan, *Journal of Materials Processing Technology* **184** (2007) 379.
5. M Hanif, M Salik, and M A Baig, *Optics and Lasers in Engineering* **49** (2011) 1456.
6. M Glowacki, *Journal of Physics* D: *Applied Physics* **28** (1995) 2051.
7. J Sabbaghzadeh, S Dadras, M J Torkamany, *Journal of Physics* D: *Applied Physics* **40** (2007) 1047.
8. M Jandaghi, P Parvin, and M J Torkamany Sabbaghzadeh, *J. Physics Procedia* **5** (2010) 107.
9. M Jandaghi, P Parvin, M J Torkamany, and J Sabbaghzadeh, *J. Phys*. D: *Appl. Phys.* **42** (2009) 205301 .
10. M Jandaghi, P Parvin, M J Torkamany, and J Sabbaghzadeh, *J. Phys*. D: *Appl. Phys.* **41** (2008) 235503.
11. S Dadras, M J Torkamany and J Sabbaghzadeh, *Optics and Lasers in Engineering* **46** (2008) 769.
12. N S HosseiniMotlagh, P Parvin, M Jandaghi, and M J Torkamany, *Optics and Laser Technology* **54** (2013) 191.
13. D H Abbott and C E Albright, *Journal of Laser Application* **6** (1994) 69.
14. B G Chung, S Rhee, and C Lee, *Materials Science and Engineering* A **272**, 2 (1999) 357.
15. U Reisgen, M Schleser, O Mokrov, and E Ahmed, *Applied Surface Science* **257** (2010) 1401.
16. J Sabbaghzadeh, M Azizi, and M J Torkamany, *Optics Laser Technology* **40** (2008) 289.
17. B Bauer, S Kralj, Z Kozuh, and L Dorn, *Mat.-wiss*. u.*Werkstofftech* **42**, 8 (2011) 718.
18. F O Borges, G H Cavalcanti, and A G Trigueiros, *Brazilian Journal of Physics* **34**, 4B (2004) 1673.
19. National Institute of Standards and Technology Database, http://physics.nist.gov/PhysRefData/ASD/lines_form.html.
20. Z Szymanski, J Kurzyna, and W Kalita, *Journal of Physics* D: *Applied Physics* **30** (1997) 3153.
21. J Wang, C Wang, X Meng, X Hu, Y Yu, and S Yu, *Optics and Laser Technology* **44** (2012) 67.
22. Y A Chang and W A Oates, "*Materials thermodynamics*", Wiley (2010).
23. F H Kaplan, *Applied Surface Science* **241** (2005) 362.
24. S Santhanakrishnan, F Kong, and R Kovacevic, *Journal of Materials Processing Technology* **211** (2012) 1247.
25. S Lu, H Fujii, and K Nogi, *Materials Science and Engineering* A **380** (2004) 290.
26. H Fujii, T Sato, S Lu, and K Nogi, *Materials Science and Engineering* A **495** (2008) 296.
27. S Lu, H Fujii, and K Nogi, *Scripta Materialia* **51** (2004) 271.
28. Y Sato, K Tomita, and T Kuwama, *Quarterly Journal of the Japan Welding Society* **10** (1992) 68.